THE JOURNAL OF PHYSICAL CHEMISTRY B

Article

pubs.acs.org/JPCB

Swelling-Induced Optical Anisotropy of Thermoresponsive Hydrogels Based on Poly(2-(2-methoxyethoxy)ethyl methacrylate): Deswelling Kinetics Probed by Quantitative Mueller Matrix Polarimetry

Nagaraj Patil,[†] Jalpa Soni,[‡] Nirmalya Ghosh,*[,‡] and Priyadarsi De*[,†]

[†]Polymer Research Centre, Department of Chemical Sciences, [‡]Department of Physical Sciences, Indian Institute of Science Education and Research, Kolkata, PO: BCKV Campus Main Office, Mohanpur-741252, Nadia, West Bengal, India

Supporting Information

ABSTRACT: Thermodynamically favored polymer−water interactions below the lower critical solution temperature (LCST) caused swelling-induced optical anisotropy (linear retardance) of thermoresponsive hydrogels based on poly(2-(2-methoxyethoxy)ethyl methacrylate). This was exploited to study the macroscopic deswelling kinetics quantitatively by a generalized polarimetry analysis method, based on measurement of the Mueller matrix and its subsequent inverse analysis via the polar decomposition approach. The derived medium polarization parameters, namely, linear retardance (δ), diattenuation (d), and depolarization coefficient (Δ), of the hydrogels showed interesting differences between the gels prepared by conventional free radical polymerization (FRP) and reversible addition−fragmentation chain transfer polymerization (RAFT) and also between dry and swollen state. The effect of temperature, cross-linking density, and polymerization technique employed to synthesize hydrogel on deswelling kinetics was systematically studied via conventional gravimetry and corroborated further with the corresponding Mueller matrix derived quantitative polarimetry characteristics (δ, d, and Δ). The RAFT gels exhibited higher swelling ratio and swelling-induced optical anisotropy compared to FRP gels and also deswelled faster at 30 °C. On the contrary, at 45 °C, deswelling was significantly retarded for the RAFT gels due to formation of a skin layer, which was confirmed and quantified via the enhanced diattenuation and depolarization parameters.

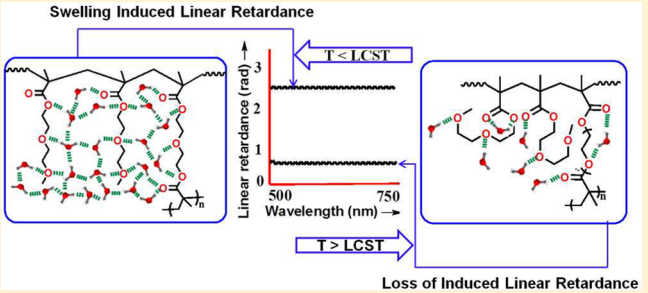

INTRODUCTION

Several stimuli-responsive polymers have been developed with the intension of mimicking biological systems, where structural and compositional gradients at different levels are essential for orderly responsive behaviors.[1,2] In this sense, hydrogels demonstrated suitability as biomedical material for medical applications.[3] Environmentally responsive hydrogels are three-dimensional, water-insoluble, water-swellable, high molecular weight networks that change their physical properties abruptly with respect to the applied external stimuli, such as temperature, light, pH, enzyme, etc.[4−7] The ability of a three-dimensional cross-linked hydrophilic network to maintain a certain degree of structural integrity and elastic stress makes them promising candidates for potential bioapplications like controlled drug delivery, enzyme recycling, protein chromatography, and tissue engineering.[8−11]

The intrinsic structure of the hydrogel network determines its volume phase transition properties, which is a direct consequence of the gelation mechanism. Gelation in conventional free-radical polymerization[12] (FRP gels) occurs via tying up of nanogel domains at a critical conversion, forming densely cross-linked nanogel domains, which are considered as structural inhomogeneities, whereas hydrogels synthesized by controlled radical polymerization[13−15] (CRP gels) are more structured and homogeneous, because gelation occurs through linking of branched and hyperbranched preformed polymers. The presence of dangling chains is the characteristic feature of the vinyl-type of network formed by CRP techniques, because branched chain ends remain in the network as dangling chains.[16] These free mobile graft chains exhibit improved molecular mobility because of greater conformational freedom.[17] Herein, reversible addition−fragmentation chain transfer (RAFT) polymerization,[18] one of the most successful CRP techniques, was used to prepare hydrogels (RAFT gels) based on 2-(2-methoxyethoxy)ethyl methacrylate (MEO_2MA). Lutz et al. demonstrated and highlighted recent advances in synthesis and application of thermoresponsive polymers and hydrogels containing short oligo(ethylene oxide methacrylate).[19] Also, short oligo(ethylene oxide methacrylate)-based monomers have been successfully copolymerized with a

Received: September 6, 2012
Revised: November 3, 2012
Published: November 6, 2012

varieties of other monomers to afford materials with diverse properties.[20]

Conventional gravimetry and image analysis[21] are widely used for studying deswelling kinetics of hydrogels, which will give little information about structural changes at various length scales, an understanding of which is vital for end user applications. Most of the studies conducted on this aspect by light, neutron and X-ray scattering techniques[22−24] have mainly considered spatial inhomogeneities in the gel. The polarization properties of light scattered from samples may yield additional microstructural functional information on complex molecular anisotropy/organization of any sample, which are otherwise hidden in polarization blind light scattering based measurements.[25] Motivated by this, polarimetric approaches have also been explored for the characterization of various types of polymers.[26,27] However, the polarization information in traditional polarimetry is measured in terms of the conventionally defined degree of polarization of light, by performing simplistic measurements of copolarized and crossed-polarized light intensity with respect to a given input polarization state of incident light or by recording selected Stokes vector elements (4×1 intensity vector describing the polarization state of light,[28] defined afterward). Semiquantitative information on the polarization properties of the sample are then extracted by employing empirical formulations on the selected polarimetry measurements. While such simpler traditional polarimetry analysis methods are suitable for optically clear media, complexities arise when several polarization events are exhibited in the sample simultaneously, that too in presence of scattering (as should be the case for hydrogels investigated in our study).[29] Simultaneous occurrences of several polarization effects contribute in a complex interrelated way to the measurable polarization signal. These therefore represent several *lumped* effects with much *interelement cross talk*, masking potentially interesting polarization metrics and hindering their unique interpretation. For extraction, quantification, and unique interpretation of the individual, intrinsic polarimetry effects of such complex systems, a more quantifiable and generally applicable technique is thus required. In the present study, we have employed such a generalized method for polarimetry analysis.

This approach is based on measurement of the Mueller matrix (a 4×4 matrix that describes the transfer function of any medium in its interaction with polarized light) and quantification of the constituent polarimetry characteristics of the medium[28−32] via inverse analysis with polar decomposition.[29,32] The Mueller matrix derived polarization parameters, namely, linear retardance (δ), diattenuation (d), and depolarization (Δ),[29,32] if separately extracted and quantified, can yield a wealth of morphological, structural, and functional information on the sample. In the present study, each of the above-mentioned intrinsic polarimetry characteristics are explored for quantitative monitoring of deswelling kinetics of the hydrogels, with early indications showing promise and warranting further explorations. To the best of our knowledge, this is the first report to correlate homogeneity with the orientation of polymer network, swelling-induced optical anisotropy, and use of such inverse polarimetry analysis methods on scattering Mueller matrices from hydrogels to investigate deswelling kinetics systematically.

EXPERIMENTAL SECTION

Experimental details including materials, synthesis and purification of linear homopolymer and hydrogels, characterization methods, fundamental equations, and definition of terms used to study deswelling kinetics by gravimetric analysis are provided in the Supporting Information.

Stokes−Mueller Algebra. The interaction of polarized light with any medium is well-described via Stokes−Mueller matrix algebra.[28−34] In this formalism, the polarization state of light is represented by four measurable intensities, known as the Stokes parameters.[30,31] The four Stokes parameters of light (I, Q, U, and V, elements of the Stokes vector $\mathbf{S}$) are represented by six intensity measurements: I is the total detected light intensity, which is the sum of the two orthogonal component intensities, Q; U and V are the differences in intensities between horizontal (0°) and vertical (90°), linear +45° and 135°, and right circular and left circular polarization states, respectively. While the Stokes vectors represent the polarization state of light, a 4×4 matrix $\mathbf{M}$, known as the Mueller matrix, describes the polarizing transfer function of any medium (contains complete information about all the medium polarization properties) in its interaction with polarized light:[30,31]

$$\mathbf{S}_o = \mathbf{M}\mathbf{S}_i \tag{1}$$

where $\mathbf{S}_i$ and $\mathbf{S}_o$ are the input and the output Stokes vectors of the light, respectively. A variety of experimental tools have been developed to measure the complete Mueller matrix of any sample.[29] We have employed an automated spectral 4×4 Mueller matrix measurement setup (Figure S1, Supporting Information), developed in house,[35] to record the Mueller matrices from the hydrogel samples (thickness ∼5 mm). The recorded Mueller matrices were then subjected to the polar decomposition analysis to yield quantitative the polarimetry characteristics d, δ, ψ, and Δ of the samples, as described below.

Inverse Polarimetry Analysis Based on Mueller Matrix Decomposition. The Mueller matrix decomposition approach consists of decomposing a given "lumped" system Mueller matrix of any unknown complex system $\mathbf{M}$ into the product of three "basis" matrices[29,32,36]

$$\mathbf{M} \Leftarrow \mathbf{M}_\Delta \cdot \mathbf{M}_R \cdot \mathbf{M}_D \tag{2}$$

Here, the matrix $\mathbf{M}_\Delta$ describes the depolarizing effects of the medium, the effects of linear and circular retardance (or optical rotation) are contained in $\mathbf{M}_R$, and $\mathbf{M}_D$ includes the effects of linear and circular diattenuation. This product decomposition process was originally proposed by Lu and Chipman for optically clear media[32] and has recently been extended to encompass complex scattering media exhibiting simultaneously many polarization and scattering effects.[36−42] Once calculated, these constituent basis matrices are further analyzed to derive individual polarization medium properties. Specifically, d, Δ, δ, and circular retardance or optical rotation (ψ, circular retardance = 2 × optical rotation), can be determined from the decomposed basis matrices. The magnitude of diattenuation (d) can be determined from $\mathbf{M}_D$ as[29,32,36]

$$d = \frac{1}{M_D(1,1)}\sqrt{M_D(1,2)^2 + M_D(1,3)^2 + M_D(1,4)^2} \tag{3}$$

Here, the coefficients $M_D(1,2)$ and $M_D(1,3)$ represent linear diattenuation for horizontal (vertical) and +45° (−45°) linear polarization, respectively, and the coefficient $M_D(1,4)$ represents circular diattenuation. Next, the net depolarization

Table 1. Synthesis and Characteristics of Hydrogels

run	gel composition	gelation time (min)	equilibrium swelling ratio[d]	linear retardance[e] (radian)	diattenuation[e]
F1	100:3:0.05[a]	15	3.4	0.024	0.012
F2	200:3:0.10[a]	23	4.7	0.021	0.013
F3	300:3:0.15[a]	31	6.0	0.031	0.042
R1	100:3:0.15:0.05[b]	108	4.4	0.022	0.031
R2	200:3:0.30:0.10[b]	156	6.5	0.061	0.060
R3	300:3:0.45:0.15[b]	255	8.6	0.124	0.084
HC	100:1:1:0.2[b]	no gel	–	0.010	0.023
LH	100:1:0.075[c]	–	–	0.008	0.020

[a][MEO_2MA]/[DEGDMA]/[AIBN]. [b][MEO_2MA]/[DEGDMA]/[CDP]/[AIBN]. [c][MEO_2MA]/[CDP]/[AIBN]. [d]Gravimetrically measured equilibrium swelling ratio at 6 °C. [e]Measured by Mueller matrix polarimetry at λ = 633 nm.

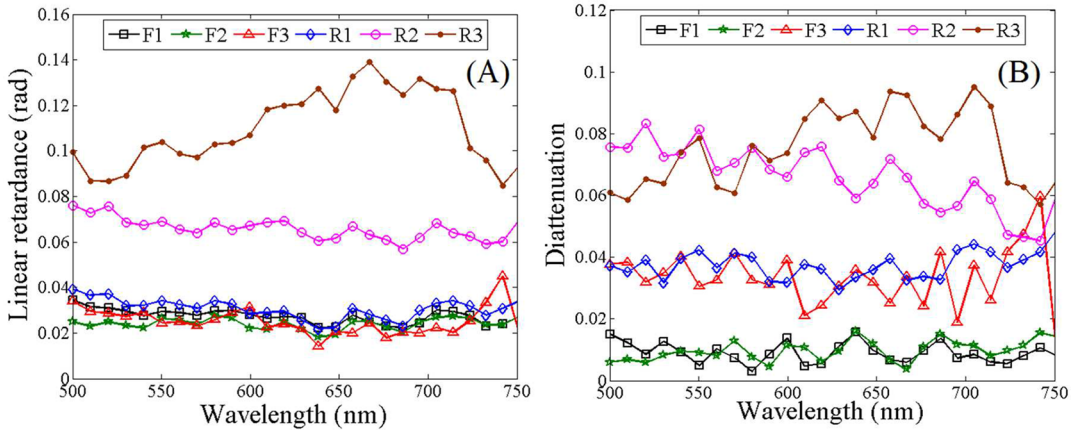

Figure 1. Comparison of (A) linear retardance and (B) diattenuation parameters as a function of wavelength for FRP and RAFT dry gels.

coefficient Δ is quantified from the depolarization matrix $\mathbf{M}_\Delta$ as[29,32,36]

$$\Delta = 1 - \frac{|\mathrm{tr}(\mathbf{M}_\Delta) - 1|}{3}, \quad 0 \le \Delta \le 1 \tag{4}$$

The magnitudes of linear retardance δ and optical rotation ψ are determined from the various elements of the decomposed retarder matrix $\mathbf{M}_R$ as[29,32,36]

$$\delta = \cos^{-1}\left(\sqrt{(M_R(2,2) + M_R(3,3))^2 + (M_R(3,2) - M_R(2,3))^2} - 1\right) \tag{5}$$

$$\psi = \tan^{-1}\left(\frac{M_R(3,2) - M_R(2,3)}{M_R(2,2) + M_R(3,3)}\right) \tag{6}$$

For the hydrogels investigated in this study, the most prominent polarimetry effects were δ, d, and Δ. None of these samples exhibited any noticeable optical rotation ψ.

RESULTS AND DISCUSSION

Synthesis. Homopolymerization of MEO_2MA (LH) was studied in *N*,*N*-dimethylformamide (DMF) solvent at 70 °C using 2,2′-azobisisobutyronitrile (AIBN) as radical source at [MEO_2MA]/[4-cyano-4-(dodecylsulfanylthiocarbonyl)-sulfanylpentanoic acid (CDP)]/[AIBN] = 100:1:0.075. During homopolymerization, monomer conversion was determined by ^{1}H NMR spectroscopy by comparing the integration of the monomer vinyl protons with the DMF protons at 8.02 ppm. We obtained a linear pseudo-first-order kinetic plot (Figure S2A, Supporting Information) and M_n increased linearly with conversion (Figure S2B, Supporting Information) with reasonable agreement between the number-average molecular weight determined ($M_{n,GPC}$) and the theoretical molecular weight ($M_{n,theo}$) calculated on the basis of conversion. Unimodal refractive index traces shifted smoothly toward lower elution volume (higher molecular weight side) with increasing monomer conversion (Figure S2C, Supporting Information). On the basis of these results, we have selected CDP as the chain transfer agent (CTA) in DMF at 70 °C to prepare RAFT hydrogels of MEO_2MA in the presence of di(ethylene glycol)dimethacrylate (DEGDMA) as cross-linker.

Hydrogels with different [monomer]/[cross-linker] ratios were prepared by FRP and RAFT polymerization (Scheme S1, Supporting Information) and results are shown in Table 1. We observed no gel formation at [CTA]/[cross-linker] = 1 (run HC, in Table 1), concluding that a high [CTA]/[cross-linker] ratio was unfavorable for the gel synthesis. Hyperbranched copolymers (HC) of MEO_2MA and DEGDMA were formed at a feed ratio of [CTA]/[cross-linker] > 0.5, which is in accordance with observations made by Liu et al.[43]

Origin of Optical Anisotropy in Hydrogel Samples. The Mueller matrices recorded from the hydrogels (wavelength range 500−750 nm) were subjected to the Mueller matrix decomposition analysis, to yield quantitative individual polarimetry parameters, namely, δ, d and Δ coefficients.[29,32] Before we describe the results of the Mueller matrix analysis, the origin of δ, d, and Δ coefficients in the hydrogels, is worth mentioning. The linear retardance is a macroscopic quantity, defined as the net phase shift between two orthogonal linear polarization states upon propagation through a medium [$\delta = (2\pi/\lambda)\Delta n \times l$; Δn is linear birefringence, λ is wavelength, and l is the path length].[29] Polymeric materials in general may exhibit linear retardance due to organization of individual anisotropic domains (originating from anisotropic molecular polarizability).

dx.doi.org/10.1021/jp308850a | J. Phys. Chem. B 2012, 116, 13913−13921

The net value of δ is determined by a number of factors, like the molecular structure, the value of (anisotropic) polarizability, easiness of lining up monomers, and the conditions of polymer synthesis. Note that even though the monomers and the cross-linkers exhibit strong molecular anisotropy, the net (observable) linear retardance may get considerably reduced due to random organization of the anisotropic domains (resulting from random orientation of the polymer chains). The effect diattenuation (which is defined as the differential attenuation of two orthogonal linear polarization states) is analogous to retardance and is also determined by organization and molecular structure.[29] The parameters affecting the net diattenuation are (i) anisotropic absorption from oriented/organized structure and (ii) scattering, reflection/transmission of light through layered structures.[29] The hydrogels investigated in our study did not show appreciable absorption in the wavelength range 500−750 nm, and thus, the latter effect is expected to be the dominant contributor to the observed diattenuation of the samples. Depolarization is primarily caused by (i) multiple scattering effects within the sample (due to the presence of turbidity) and (ii) randomly oriented spatial domains of birefringent structures.[29,30] From the Mueller matrix point of view, the latter effect can be understood by noting that incoherent addition of pure retardance Mueller matrices having random orientation of retardation axes leads to the Mueller matrix corresponding to a pure depolarizer.[29,30] Having described the plausible origin of the three most prominent polarimetry effects, we now turn to the results of the Mueller matrix decomposition results of the hydrogels. Figure 1 shows the wavelength variation of the Mueller matrix decomposition-derived δ and d parameters, respectively, for both the FRP and RAFT dry gels. Note that typical Mueller matrix elemental error of our experimental polarimetry system is $\sim\pm0.01$ (see ref 35 for details), which should lead to uncertainties in the absolute values of the derived δ and d parameters $\leq\pm0.02$. Thus, the variations of δ and d parameters presented in Figure 1 and in other subsequent figures are typically associated with uncertainties of $\sim\pm0.02$.

Several interesting trends can be gleaned from Figure 1. Both FRP and RAFT dry gels exhibited appreciable linear retardance and diattenuation effects, whereas the corresponding linear homopolymer of MEO_2MA (run LH in Table 1) and hyperbranched copolymer of MEO_2MA with DEGDMA (run HC in Table 1) did not exhibit any significant linear retardance and diattenuation effects ($\delta \sim 0.01$ rad, $d \sim 0.02$, not shown here). Nonlinearity of oligo(ethylene glycol) (OEG) analogues and large segmental mobilities associated with polymer chains may cause increased randomization of chains, leading to reduction of the net linear retardance and diattenuation effects for these. The organization of pore structures[44] and suppression of segmental mobilities of polymer chains in the gel due to significant spatial restrictions (cross-linking reactions) minimize polymer chain randomization, which may lead to appreciable retardance and diattenuation effects. However, the magnitudes of δ and d parameters were observed to be higher for the RAFT (R3 > R2 > R1) gels compared to the FRP gels with similar composition. This can be attributed to the difference in the network structure, decided by the mechanism of gelation, as explained in the Introduction. Another easily observable parameter that indicates the network structure of hydrogel is gelation time. It is obvious from Table 1 that the gelation time of FRP hydrogels was shorter than that of RAFT hydrogels. Longer gelation time for R3 could be explained by the retardation effect offered by a high concentration of CTA, ensuring more and more intermolecular cross-linking reactions, by slowing down the reaction rate and hence yielding a more structured network (Figure 1, Table 1).

Swelling Induced Optical Anisotropy of Hydrogels. The swollen gels exhibited much stronger linear retardance and diattenuation effects compared to the dry gels. For example, the value for δ (at λ = 633 nm) of the swollen F2 and R2 are $\delta \sim$ 1.8 and 2.2 rad, respectively (Figure S3A, Supporting Information), as compared to the corresponding values of $\delta \sim$ 0.02 rad (F2) and 0.06 rad (R2), for the dry gels. The significantly higher magnitude of δ in the swollen gels can be attributed to the fact that, in the extended conformation, well-exposed ethereal oxygen atoms of the OEG pendant groups provide hydrogen-bonding sites where water molecules localize and serve as nucleating sites for formation of highly cooperative large water clusters (hydration shell).[45] These water clusters effectively polarize the ethereal oxygen atoms of OEG, thereby increasing molecular polarizability, whereas apolar carbon−carbon backbone and terminal methyl groups lead to a competitive hydrophobic effect. The extended network of OEG−water, water−water hydrogen bonds throughout the gel induces structuring of water molecules around ethereal oxygen atoms, polymer backbone, and more importantly around the terminal methyl groups, forming water cage structures. When a hydrophobic molecule is added to water, water molecules bind together to enhance the structural order, resulting in a negative entropy of mixing (hydrophobic hydration).[46] This hydration causes alignment of nonlinear OEG analogues due to bridging of water molecules between neighboring pendant groups and also between the random networks and hence throughout the gel. Thus, the more extended and relaxed polymer network can have a well-aligned and organized anisotropic domain, which is manifested as a stronger linear retardance effect in the swollen gels, termed as swelling-induced optical anisotropy (linear retardance). Since the RAFT gels were more homogeneous and well structured as compared to the FRP gels, the swelling ratios (Table 1) and the swelling-induced optical anisotropy (Figure S3A, Supporting Information) were significantly enhanced for the RAFT gels.

Note that although the diattenuation parameter also showed a similar variation as that of retardance, there exist subtle but important differences in the origin of the diattenuation and the retardance effects. While retardance primarily arises due to the presence of organized anisotropic domains, diattenuation is also strongly influenced by formation of organized *layered* structures. The higher d values for the RAFT gels compared to the FRP gels (specifically for the swollen gels, where the effect is much more pronounced compared to the dry gels; see Figures 1B and S3B, Supporting Information) thus signify the presence of a more layered structural arrangement of networks in the RAFT gels due to the presence of a uniform network structure.

Gravimetric Deswelling Kinetics. Equilibrium swelling ratios measured at 6 °C (below LCST) by gravimetry are shown in Table 1. Among gels with the same feed ratio, RAFT gels have shown a higher swelling ratio than FRP gels, which can be attributed to more structural homogeneity (Table 1) because of reduced formation of collapsed nanogel domains.[47] As-synthesized FRP gels remained clear and transparent in DMF as well as in water. In contrast, RAFT gels had the characteristic yellow color in DMF, and their appearance changed when they were immersed in water. The clarity and

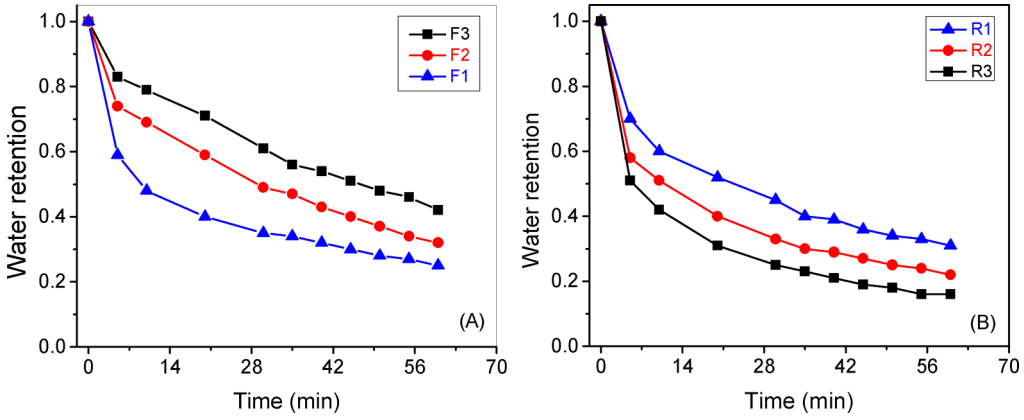

Figure 2. Comparison of water retention upon deswelling at 30 °C between (A) FRP and (B) RAFT gels of different cross-linker densities.

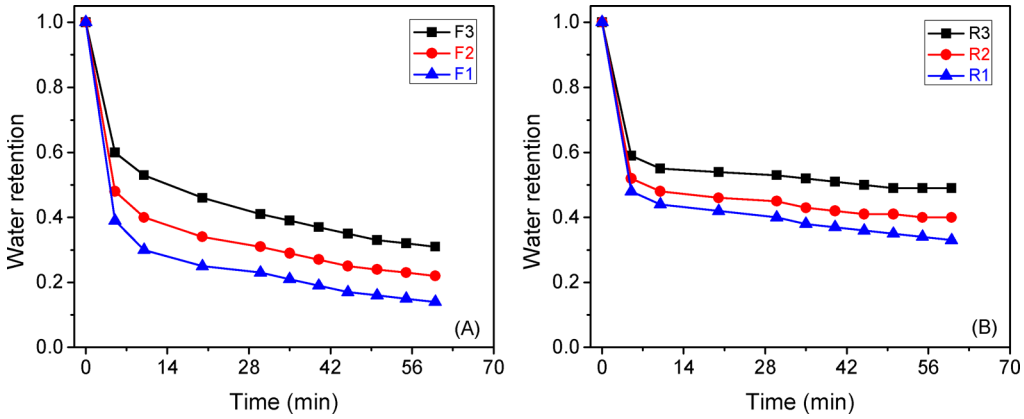

Figure 3. Comparison of water retention upon deswelling at 45 °C between (A) FRP and (B) RAFT gels of different cross-linker densities.

transparency of gels decreased with increased [CTA]/[cross-linker] ratio. The turbidity of RAFT gels in water is a consequence of the existence of abundant dangling chains.[17]

Deswelling kinetics of hydrogels above LCST was studied at 30 and 45 °C by recording the decrease of weight as a function of time by conventional gravimetry, which was converted to the decrease of water retention (eq 2, Supporting Information). The decrease of water retention against time for FRP and RAFT gels with different cross-linker densities at 30 °C is shown in Figure 2. The gel F1 shrank fast and lost 65% of water within 30 min (see Figure 2A), whereas deswelling of F3 was the slowest, with 39% of water lost within 30 min, and deswelling of F2 was intermediate. It was observed that the rate of deswelling of FRP gels increased with the [cross-linker]/[monomer] ratio, in accordance with the increase of densely cross-linked nanogel domains and hence heterogeneity.[16] These nanogel domains retain their hydrophilic property during phase transition for a longer time, which will provide a hydrophilic channel for water molecules to diffuse out.[16]

The RAFT gels showed accelerated deswelling kinetics compared to FRP gels at 30 °C (Figure 2B). The R3, R2, and R1 lost 75, 67, and 55% of water within 30 min, respectively. This reverse trend compared to FRP gels could be explained by understanding the gelation mechanism. The gelation by CRP occurs through random cross-linking of preformed branched and hyperbranched chains with reduced formation of nanogel domains.[48] The presence of dangling chains, which show rapid dehydration followed by subsequent hydrophobic intermolecular aggregation of dehydrated grafted chains, improves molecular mobility. These dehydrated graft chains create hydrophobic cores, which can enhance the hydrophobic aggregation of the networks, resulting in acceleration of shrinking kinetics. The accelerated rate of deswelling of RAFT gels was proportional to [CTA]/[cross-linker], in accordance with an increase in the number of dangling chains introduced by the RAFT agent, which would accelerate the hydrophobic aggregation force, forming water leakage channels for water molecules to diffuse out through generated cracks. Hence, R3 deswelled faster than R2 than R1.

Near LCST (30 °C), R2 and R3 gels deswelled faster, respectively, compared to F2 and F3 gels, which matches well with the literature results.[16,17,49] However, F1 deswelled faster than R1. This could be due to the very low concentration of CDP needed to introduce a sufficient number of dangling chains in R1 and/or the high heterogeneity of F1. It was expected that the rate of deswelling should increase with temperature, and this was true for FRP gels. FRP gels deswelled faster at 45 °C (Figure 3A) compared at 30 °C, where in contrast RAFT gels deswelled slower and the order was reversed; i.e., R1 deswelled faster than R2 and R2 faster than R3 (Figure 3B). At elevated temperature (45 °C) volume phase transitions are relatively fast, resulting in rapid dehydration of chains situated at the water−gel interface, followed by faster hydrophobic aggregation to form a surface-dense, thick skin layer, which is impermeable to water molecules, thereby, retarding the deswelling rate because water molecules have to leak through generated cracks after rupturing of the skin layer. The skin layer forming ability depends on temperature, method

dx.doi.org/10.1021/jp308850a | J. Phys. Chem. B 2012, 116, 13913−13921

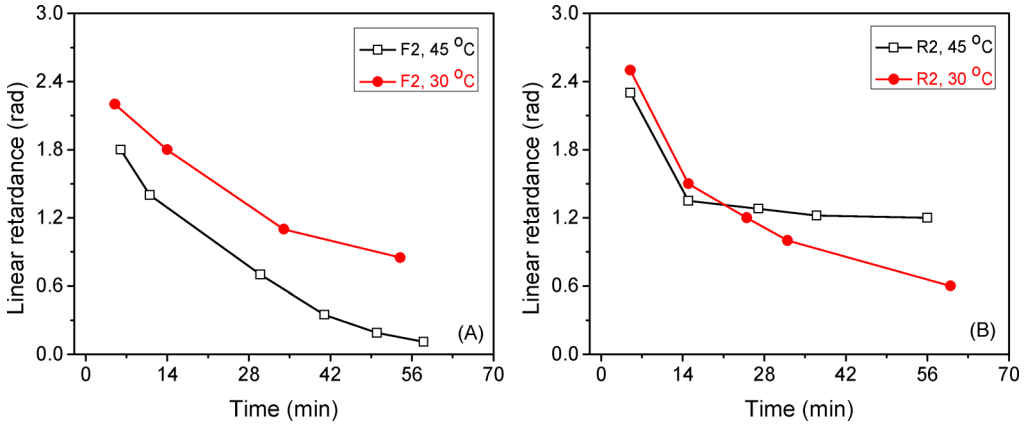

Figure 4. Variation of linear retardance as a function of time upon deswelling for (A) F2 gel and (B) R2 gel at 30 and 45 °C.

of polymerization to produce the gel, and also cross-linker density. As established in the earlier sections, the structure and homogeneity of RAFT gels was proportional to the [monomer]/[cross-linker] ratio; hence, gel R3 was more homogeneous, had less cross-linker density, as a result being more vulnerable to form a skin layer,[16] and consequently deswelled slowly at 45 °C compared to R2 and R1. In contrast, FRP gels deswelled faster at 45 °C due to the inherent heterogeneity associated with FRP gels; they were not affected by a skin layer, and as a result their deswelling was guided by [cross-linker]/[monomer] at any temperature above the LCST. An increase in temperature increases the hydrophobic aggregation force, leading to accelerated shrinking kinetics.

Monitoring Deswelling Kinetics by Mueller Matrix Polarimetry. The marked difference between the values of Mueller matrix decomposition derived δ and d parameters among dry and swollen gels contains complementary and useful information, which may be exploited for quantitative monitoring of structural changes in hydrogels during deswelling. This was therefore explored by monitoring the Mueller matrix derived parameters at λ = 633 nm. Since none of the decomposition-derived polarization parameters exhibited any distinct spectral characteristics, rather the spectral variation were quite broad and gradual, the choice of the λ was not that critical for this purpose.

The variation of δ with time for swollen F2 and R2 gels are shown in Figure 4, parts A and B, respectively. For the F2 gel (Figure 4A), the value for δ at a given time was found to be lower and also decayed faster with time at 45 °C compared to that at 30 °C. This can be explained as follows. As the temperature increased above LCST, loosely bound water molecules situated at the surface of hydrophobic regions (free water) diffuses out rapidly due to the increase of entropic penalty, which randomizes the polymer networks. This accounts for the observed rapid fall of linear retardance with time during the early period of deswelling (weakening of the hydrogen-bonded network due to the lack of free water), followed by gradual loss of bridged water molecules.[50] The system entropy would be increased due to cooperative polar dehydration and subsequent formation of a collapsed hydrophobic cluster resulting from diffusion of the hydrophobic group's hydration shell into the bulk which is further stabilized by coalesce of adjacent hydrophobic pockets (which can be considered as heterogeneities) via hydrophobic interactions.[51] The increased hydrophobic aggregation force and hence rapid accumulation of hydrophobic pockets lead to more rapid loss of swelling-induced structures and linear retardance (this phenomenon is represented pictorially in Scheme 1) for the

Scheme 1. Cartoon Representation of Swelling-Induced Structuring and Loss of Induced Structure (Linear Retardance/Optical Anisotropy) During Deswelling

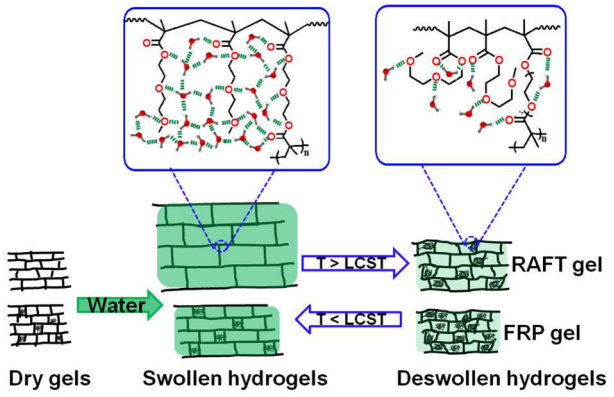

F2 gels at 45 °C as compared to that at 30 °C. Interestingly, the variation of δ with time for the R2 gel was observed to be slower and almost attained an equilibrium value at 45 °C as compared to that at 30 °C. Contrary to the deswelling of F2 gel at 30 and 45 °C and also R2 at 30 °C, the retention of linear retardance was observed to be much more pronounced for the R2 gel at 45 °C (Figure 4B), which arises due to a significant penetration of water into the interior of the collapsed gel, as supported by 40% of water retention measured by gravimetry (Figure 3B). This possibly originates due to the formation of impermeable surface dense skin layers at 45 °C, which can be confirmed and quantified by the diattenuation parameter, as described below. Thus, the nature of the variation of δ with time is a clear manifestation of the underlying deswelling phenomenon.

The variation of diattenuation with time for swollen F2 and R2 gels are shown in Figure 5, parts A and B, respectively, at 30 and 45 °C. Due to collapsing of the polymer network during deswelling, the organized layer structure could be disturbed; accordingly, the value for d decreases with time. The variations of diattenuation for the F2 gel at 30 and 45 °C (Figure 5A) were qualitatively similar to those observed for linear retardance (Figure 4A), for reasons described previously. Importantly, for the R2 gel, the magnitude of diattenuation was found to be considerably higher at 45 °C and was also observed to decay

dx.doi.org/10.1021/jp308850a | J. Phys. Chem. B 2012, 116, 13913−13921

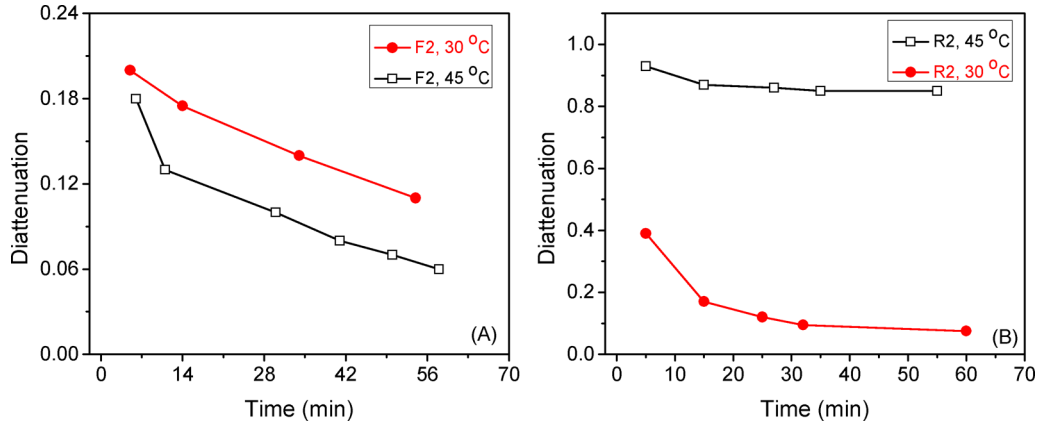

Figure 5. Variation of diattenuation as a function of time upon deswelling for (A) F2 gel and (B) R2 gel at 30 and 45 °C.

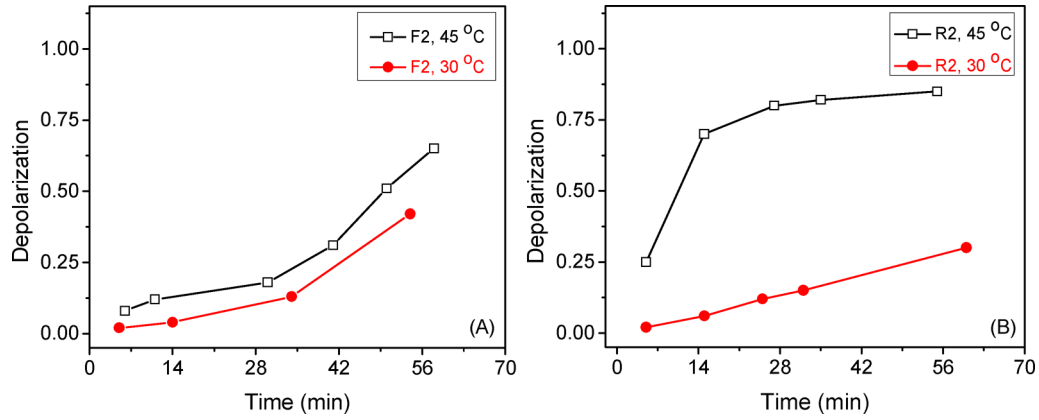

Figure 6. Variation of depolarization as a function of time upon deswelling for (A) F2 gel and (B) R2 gel at 30 and 45 °C.

much more slowly with time, as compared to that observed at 30 °C. As noted previously, this arises because of formation of a skin layer at the water−gel interface, which hindered further water release. This is therefore in conformity with the hypothesis of surface-dense skin layer formation (derived from the results presented in Figures 4B and S3B, Supporting Information).

In Figure 6, we show the variation of the Mueller matrix decomposition derived depolarization coefficient (Δ) with time for swollen F2 and R2 gels. As noted previously, the two competing process for the observed depolarization are turbidity-induced multiple scattering effects and randomization of the orientation of spatial domains of birefringent structures.[29] A clear manifestation of these two competing processes can be observed in the variation of Δ for the F2 gel (Figure 6A). The initial gradual increase of Δ with time can be attributed to polarization loss due to randomization of organized spatial birefringent domains.[29] As expected, in this region, the variation of Δ shows a correlated behavior to that observed for δ (Figure 4A), where Δ increased gradually till it lost ∼50% of linear retardance at 30 °C and ∼65% at 45 °C. The value for Δ then shows a more rapid increase, which arises due to the additional contribution of depolarization due to multiple scattering effects. This follows because increased hydrophobic−hydrophobic aggregations and collapsed polymer networks lead to the formation of clusters of hydrophobic pockets, in turn giving rise to appreciable multiple scattering effects. Since this effect was more pronounced at higher temperature (45 °C), the rate of change of Δ was also accordingly found to be more pronounced at 45 °C (Figure 6A).

For the R2 gel at 30 °C, the value for depolarization coefficient Δ remained low and increased slowly with time (Figure 6B). This is in agreement with the corresponding variation of linear retardance and diattenuation (Figures 4B and 5B), which is indicative of a lesser possibility of formation of a skin layer and hence an accelerated deswelling process. In contrast to this, at 45 °C, after 15 min of deswelling, the value for Δ abruptly increased to a very high value (Figure 6B). In fact, the gel became completely turbid with the formation of bubbles containing water on the surface due to formation of a skin layer (as indicated by the corresponding magnitude of diattenuation in Figure 5B), leading to a very strong depolarization effect.

Attempts were further made to explore quantitative information and insight into the structural changes occurring in the hydrogels during deswelling. For this purpose, the dependence of the δ on the absolute amount of absorbed water was quantified and analyzed, by taking out the gel from the measurement bath and weighing it quickly, converting the weight of the sample to water loss (eq 3 of the Supporting Information). Since both the value for δ and water retention were observed to decay with the time, when the values for δ are plotted against water loss, a linear dependence was observed (Figure S4, Supporting Information). By estimating the value of the coefficient of the slope for the δ against water loss curve, one can quantitatively describe deswelling kinetics. As one would expect, a larger value of the estimated slope coefficient

dx.doi.org/10.1021/jp308850a | J. Phys. Chem. B 2012, 116, 13913−13921

indicates faster deswelling. The values for the slopes obtained from the δ vs water loss curve are listed in Table S1 (Supporting Information). As is obvious, at 30 °C, R2 deswelled faster than F2, and the trend was reversed at 45 °C. Thus, the results presented above demonstrate that the intrinsic polarization parameters of the hydrogel matrices contain complementary and useful information on the structural changes during the deswelling process.

CONCLUSIONS

RAFT polymerization of MEO_2MA with DEGDMA was successfully conducted using CDP as CTA to afford a well-defined and structured network with different cross-linker density compared to FRP gels. RAFT gels with higher [monomer]/[cross-linker] or [CTA]/[cross-linker] ratios demonstrated higher swelling ratios compared to FRP gels with similar composition, due to formation of reduced nanogel domains. Moreover, these RAFT gels also showed accelerated deswelling kinetics at 30 °C, because of an increased number of dangling chains introduced by CTA. This accelerated deswelling was quantified via the observed sharper decay of the Mueller matrix derived linear retardance δ parameter. In contrast, at 45 °C, the deswelling was observed to be significantly retarded for the RAFT gels (as indicated by considerably slower decay of δ). This was identified to originate due to the formation of impermeable surface dense skin layers at the water−gel interface, the formation of which was manifested as an enhancement of the diattenuation d and depolarization Δ parameters. Simultaneous measurement, quantification, and interpretation of the polarization parameters, in terms of the organization of the anisotropic domains, formation of layered structures, and turbidity of the complex hydrogel matrix, are exclusively enabled by the Mueller matrix inverse polarimetry analysis method. Note that none of these trends from such complex systems (hydrogel matrix exhibiting several simultaneous polarization and scattering events) can be gleaned from conventional light scattering and traditional polarimetry analysis, where at best one would have to resort to semiempirical formulations for qualitative information. These Mueller matrix decomposition derived polarimetry parameters thus hold promise as useful sample metrics for quantitative monitoring of deswelling kinetics of hydrogels, and initial application of this approach shows promise and warrants further explorations. In general, this novel Mueller matrix inverse analysis method may open the door for polarimetric characterization of polymer samples for a variety of applications, of which we have illustrated an important example.

ASSOCIATED CONTENT

Supporting Information

Additional information as noted in the text. This material is available free of charge via the Internet at http://pubs.acs.org.

AUTHOR INFORMATION

Corresponding Author

*E-mail: p_de@iiserkol.ac.in (P.D.), nghosh@iiserkol.ac.in (N.G.).

Notes

The authors declare no competing financial interest.

ACKNOWLEDGMENTS

This work was supported by the Indian Institute of Science Education and Research—Kolkata and the Department of Science and Technology (DST), New Delhi, India [Project No.: SR/S1/OC-51/2010].

REFERENCES

(1) Liu, F.; Urban, M. W. *Prog. Polym. Sci.* **2010**, *35*, 3−23.
(2) Geckil, H.; Xu, F.; Zhang, X.; Moon, S. J.; Demirci, U. *Nanomedicine* **2010**, *5*, 469−484.
(3) Peppas, N. A.; Hilt, Z. J.; Khademhosseini, A.; Langer, R. *Adv. Mater.* **2006**, *18*, 1345−1360.
(4) Peppas, N. A.; Khare, A. R. *Adv. Drug Delivery Rev.* **1993**, *11*, 1−35.
(5) Gong, C.; Wong, K. L.; Lam, M. H. W. *Chem. Mater.* **2008**, *20*, 1353−1358.
(6) Popescu, M. T.; Mourtas, S.; Pampalakis, G.; Anstimisiaris, S. G.; Tsitsilianis, C. *Biomacromolecules* **2011**, *12*, 3023−3030.
(7) Huang, X.; Lowe, T. L. *Biomacromolecules* **2005**, *6*, 2131−2139.
(8) Zimmerberg, J.; Chernomordik, L. V. *Adv. Drug Delivery Rev.* **1999**, *31*, 197−221.
(9) Groger, H.; Capan, E.; Barthuber, A.; Vorlop, K. D. *Org. Lett.* **2001**, *3*, 1969−1972.
(10) Kim, J. J.; Park, K. *Bioseparation* **1999**, *7*, 177−184.
(11) Nimmo, C. M.; Owen, S. C.; Shoichet, M. S. *Biomacromolecules* **2011**, *12*, 824−830.
(12) Xue, W. H.; Malcolm, B. J.; Timothy, G. J. *Eur. Polym. J.* **2005**, *41*, 239−248.
(13) Ide, N.; Fukuda, T. *Macromolecules* **1999**, *32*, 95−98.
(14) Yoon, J. A.; Kowalewski, T.; Matyjaszewski, K. *Macromolecules* **2011**, *44*, 2261−2268.
(15) Liu, B.; Kazlauciunas, A.; Guthrie, J. T.; Perrier, S. *Macromolecules* **2005**, *38*, 2131−2136.
(16) Yoon, J. A.; Chakicherla, G.; Gil, Roberto, R.; Kowalewski, T.; Matyjaszewski, K. *Macromolecules* **2010**, *43*, 4791−4797.
(17) Qunfeng, L.; Zhang, P.; Qing, A.; Lan, Y.; Lu, M. *Polymer* **2006**, *47*, 2330−2336.
(18) Chiefari, J.; Chong, Y. K.; Ercole, F.; Krstina, J.; Jeffery, J.; Le, T. P. T.; Mayadunne, R. T. A.; Meijs, G. F.; Moad, C. L. G.; Rizzardo, M. E.; Thang, S. H. *Macromolecules* **1998**, *31*, 5559−5562.
(19) (a) Lutz, J.-F.; Akdemir, O.; Hoth, A. *J. Am. Chem. Soc.* **2006**, *128*, 13046−13047. (b) Lutz, J.-F.; Hoth, A. *Macromolecules* **2006**, *39*, 893−896. (c) Lutz, J.-F. *J. Polym. Sci., Part A: Polym. Chem.* **2008**, *46*, 3459−3470. (d) Lutz, J.-F. *Adv. Mater.* **2011**, *23*, 2237−2243.
(20) (a) Pal, S.; De, P. *Chem. Commun.* **2012**, *48*, 4229−4231. (b) Liras, M.; García-García, J. M.; Quijada-Garrido, I.; Gallardo, A.; París, R. *Macromolecules* **2011**, *44*, 3739−3745. (c) París, R.; Quijada-Garrido, I. *Eur. Polym. J.* **2010**, *46*, 2156−2163.
(21) Nilsson, P.; Hansson, P. *J. Colloid Interface Sci.* **2008**, *325*, 316−323.
(22) Rouf, C.; Bastide, J.; Pujol, J. M.; Schosseler, F.; Munch, J. P. *Phys. Rev. Lett.* **1994**, *73*, 830−833.
(23) Shibayama, M.; Suetoh, Y.; Nomura, S. *Macromolecules* **1996**, *29*, 6966−6968.
(24) Barretta, P.; Bordi, F.; Rinaldi, C.; Paradossi, G. *J. Phys. Chem. B* **2000**, *104*, 11019−11026.
(25) Jirgensons, B. *Optical Rotatory Dispersion of Proteins and Other Macromolecules*; Springer-Verlag, 1960.
(26) Butler, M. F.; Butler, M. H. *Biomacromolecules* **2003**, *4*, 928−936.
(27) Zhang, Q.; Archer, L. A. *Macromolecules* **2004**, *37*, 1928−1936.
(28) Kliger, D. S.; Lewis, J. W.; Randall, E. *Polarized Light in Optics and Spectroscopy*; Academic Press−Harcourt Brace Jovanovich: New York, 1990.
(29) Ghosh, N.; Vitkin, A. I. *J. Biomed. Opt.* **2011**, *16*, 110801 (1−29).
(30) Chipman, R. A. In *Handbook of Optics*, 2nd ed.; Bass, M.; Ed.; McGraw-Hill: New York, 1994; Vol. 2, Chapter 22, pp 22.1−22.37.

(31) Bickel, W. S.; Bailey, W. M. *Am. J. Phys.* **1985**, *53*, 468−478.
(32) Lu, Y. S.; Chipman, R. A. *J. Opt. Soc. Am. A* **1996**, *13*, 1106−1113.
(33) Michl, J.; Thulstrup, E. W. *Spectroscopy with Polarized Light*; VCH: New York, 1986.
(34) Browne, C. B.; Zerban, F. W. *Physical and Chemical Methods of Sugar Analysis*; Wiley: New York, 1941.
(35) Purwar, H.; Soni, J.; Lakhotia, H.; Chandel, S.; Banerjee, C.; Ghosh, N. *Proc. SPIE* **2012**, *8230*, 823019−823033.
(36) Ghosh, N.; Wood, M. F. G.; Vitkin, A. I. *J. Biomed. Opt.* **2008**, *13*, 044036(1−14).
(37) Ghosh, N.; Wood, M.; Vitkin, A. I. In *Handbook of Photonics for Biomedical Science*; Valery, V. T., eEd.; Taylor and Francis Publishing: 2010; Chapter 9.
(38) Soni, J.; Purwar, H.; Ghosh, N. *Opt. Commun.* **2011**, *285*, 1599−1607.
(39) Ghosh, N.; Wood, M.; Vitkin, A. I. *Opt. Commun.* **2010**, *283*, 1200−1208.
(40) Ghosh, N.; Wood, M.; Vitkin, A. I. *J. Appl. Phys.* **2009**, *105*, 102023−102028.
(41) Ghosh, N.; Wood, M.; Li, S.; Weisel, R. D.; Wilson, B. C.; Li, R.; Vitkin, A. I. *J. Biophotonics* **2009**, *2*, 145−156.
(42) Wood, M.; Ghosh, N.; Wallenburg, M. A.; Li, S.; Weisel, R.; Wilson, B. C.; Li, R.; Vitkin, A. I. *J. Biomed. Opt.* **2010**, *15*, 047009(1−9).
(43) Liu, B.; Kazlauciunas, A.; Guthrie, J. T.; Perrier, S. *Macromolecules* **2005**, *38*, 2131−2136.
(44) Millon, L. E.; Nieh, M. P.; Hutter, J. L.; Wan, W. *Macromolecules* **2007**, *40*, 3655−3662.
(45) Ludwig, R. *Angew. Chem., Int. Ed.* **2001**, *40*, 1808−1827.
(46) Nemethy, G.; Scheraga, H. A. *J. Chem. Phys.* **1962**, *36*, 3382−3400.
(47) Doura, M.; Naka, Y.; Aota, H.; Matsumoto, A. *Macromolecules* **2005**, *38*, 5955−5963.
(48) Doura, M.; Naka, Y.; Aota, H.; Matsumoto, A. *Macromolecules* **2003**, *36*, 8477−8482.
(49) Lutz, J.-F.; Weichmann, K.; Akdemir, O.; Hoth, A. *Macromolecules* **2007**, *40*, 2503−2508.
(50) Sekine, Y.; Fukazawa, T. I. *J. Chem. Phys.* **2009**, *130*, 034501 (1−7).
(51) Ono, Y.; Shikata, T. *J. Am. Chem. Soc.* **2006**, *128*, 10030−10031.